Inorganic Chemistry

ARTICLE

pubs.acs.org/IC

Artificial Amino Acids in Nickel(II) and Nickel(II)/Lanthanide(III) Chemistry

Tereza Peristeraki,[†] Marianna Samios,[†] Milosz Siczek,[‡] Tadeusz Lis,[‡] and Constantinos J. Milios*[,†]

[†]Department of Chemistry, The University of Crete, Voutes, 71003 Herakleion, Greece

[‡]Faculty of Chemistry, The University of Wroclaw, Joliot-Curie 14, 50-383 Wroclaw, Poland

Supporting Information

ABSTRACT: The synthesis and magnetic properties of five new homo- and heterometallic nickel(II) complexes containing artificial amino acids are reported: $[Ni_4(aib)_3(aibH)_3(NO_3)](NO_3)_4\cdot 3.05MeOH$ (**1**·3.05MeOH), $[Ni_6La(aib)_{12}](NO_3)_3\cdot 5.5H_2O$ (**2**·5.5H_2O), $[Ni_6Pr(aib)_{12}](NO_3)_3\cdot 5.5H_2O$ (**3**·5.5H_2O), $[Ni_5(OH)_2(L\text{-aba})_4(OAc)_4]\cdot 0.4EtOH\cdot 0.3H_2O$ 6(**4**·0.4EtOH·0.3H_2O), and $[Ni_6La(L\text{-aba})_{12}][La_2(NO_3)_9]$ (**5**; aibH = 2-aminoisobutyric acid; L-abaH = L-2-aminobutyric acid). Complexes **1** and **4** describe trigonal-pyramidal and square-based pyramidal metallic clusters, respectively, while complexes **2**, **3**, and **5** can be considered to be metallocryptand-encapsulated lanthanides. Complexes **4** and **5** are chiral and crystallize in the space groups *I*222 and $P2_13$, respectively. Direct-current magnetic susceptibility studies in the 2−300 K range for all complexes reveal the presence of dominant antiferromagnetic exchange interactions, leading to small or diamagnetic ground states.

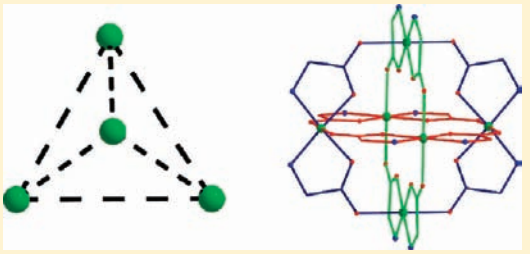

INTRODUCTION

Over the past few years, the synthesis of polymetallic clusters has attracted enormous interest because of the applications that such species present in various fields of science and technology.[1] One of the most intriguing developments in molecular magnetism is the discovery that simple coordination compounds of paramagnetic metal ions can function as nanomagnets at low temperatures in the absence of an external magnetic field, retaining their magnetization once magnetized.[2] This phenomenon, which has been termed single-molecule magnetism, was initially investigated for 3d metals such as manganese and iron and has now been expanded to include all other d- and f-block metal ions.[3] F-block ions such as the lanthanides are the most recent addition to the single-molecule magnet (SMM) family with examples of lanthanide-only clusters, including single-ion complexes, exhibiting slow relaxation of the magnetization at low temperatures. This is also true for the 3d−4f heterometallic clusters because such species represent excellent candidates for displaying enhanced magnetic properties.[4] In order for a cluster to display SMM behavior, two criteria must be met, namely, a large spin ground state, *S*, and a large negative magnetoanisotropy, *D*. That justifies why lanthanides are considered to be central players in the SMM field; the magnitude of the spin and the magnetic anisotropy of the lanthanides provide good starting "ingredients" for the synthesis of SMMs.

An important future development for the 3d−4f SMM field is the discovery of new synthetic schemes that can yield new molecules and families of related molecules with large spins and/or significant values of magnetoanisotropy. With the above in mind, we initiated a project to examine the synthetic systems of Ni^{2+}/Ln^{3+}/aibH and Ni^{2+}/Ln^{3+}/L-abaH, where aibH is 2-aminoisobutyric acid and L-abaH is L-2-aminobutyric acid (Scheme 1). Herein we report the syntheses, structures, and magnetic properties of five new homo- and heterometallic clusters built with these artificial amino acids.

EXPERIMENTAL SECTION

All manipulations were performed under aerobic conditions, using materials as received.

$[Ni_4(aib)_3(aibH)_3(NO_3)](NO_3)_4\cdot 3.05MeOH$ (1·3.05MeOH). Method 1: To a stirred solution of $Ni(NO_3)_2\cdot 6H_2O$ (292 mg, 1 mmol) and $La(NO_3)_3\cdot 6H_2O$ (177 mg, 0.5 mmol)) in MeOH (30 mL) was added aibH (103 mg, 1 mmol). The resulting pale-green solution was left to stir for 45 min, during which time it did not change color. The solution was then filtered and layered with Et_2O (40 mL). Pale-green crystals of **1**·3.05MeOH formed over 2 days in ∼40% yield. Anal. Calcd (found) for **1**: C, 26.37 (26.45); H, 5.42 (5.24); N, 11.67 (11.72).

$[Ni_6La(aib)_{12}](NO_3)_3\cdot 5.5H_2O$ (2·5.5H_2O). To a stirred solution of $Ni(NO_3)_2\cdot 6H_2O$ (292 mg, 1 mmol), $La(NO_3)_3\cdot 6H_2O$ (177 mg, 0.5 mmol), and aibH (103 mg, 1 mmol) in MeOH (30 mL) was added NEt_3 (2 mmol). The resulting pale-green solution was left to stir for 45 min, during which time the solution turned pink. The solution was then filtered and allowed to evaporate slowly. Pink crystals of **2**·5.5H_2O formed over 2 days in ∼45% yield. Anal. Calcd (found) for **2**: C, 30.30 (30.36); H, 5.09 (4.93); N, 11.04 (11.09).

$[Ni_6Pr(aib)_{12}](NO_3)_3\cdot 5.5H_2O$ (3·5.5H_2O). Complex **3** was synthesized according to the procedure followed for **2**. Yield: ∼55%.

Received: March 8, 2011
Published: April 27, 2011

Scheme 1. Structures of aibH and L-abaH and Their Coordination Modes in 1−5

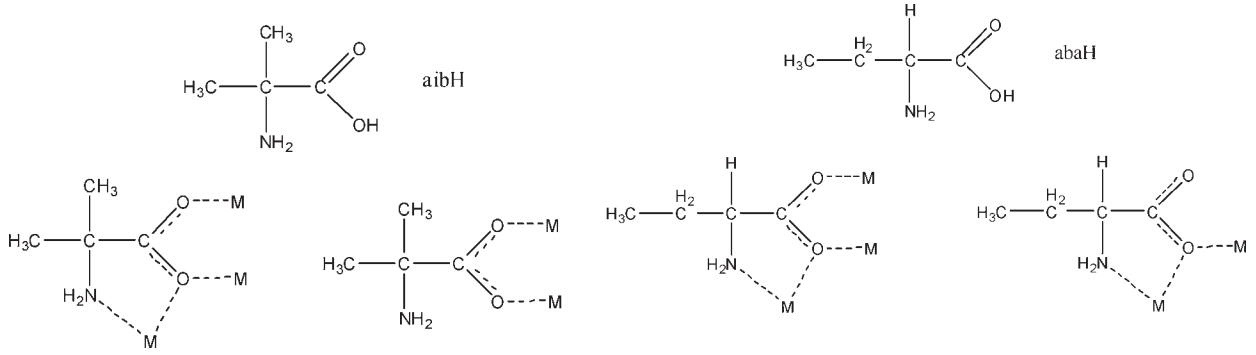

Anal. Calcd (found) for **3**: C, 30.27 (30.35); H, 5.08 (4.90); N, 11.03 (11.12).

$[Ni_5(OH)_2(L\text{-aba})_4(OAc)_4]\cdot 0.4EtOH\cdot 0.3H_2O$ (4·0.4EtOH·0.3H$_2$O). To a stirred solution of $Ni(OAc)_2\cdot 4H_2O$ (245 mg, 1 mmol) and $La(NO_3)_3\cdot 6H_2O$ (177 mg, 0.5 mmol) in EtOH (30 mL) was added L-abaH (103 mg, 1 mmol). The resulting pale-green solution was left to stir for a further 45 min, during which time it did not change color. The solution was then filtered and layered with Et_2O (40 mL). Pale-green crystals of **4** formed over 2 days in ∼25% yield. Anal. Calcd (found) for **4**: C, 30.14 (30.25); H, 5.25 (5.34); N, 5.41 (5.29).

$[Ni_6La(L\text{-aba})_{12}][La_2(NO_3)_9]$ (5). To a stirred solution of $Ni(OAc)_2\cdot 4H_2O$ (245 mg, 1 mmol), $La(NO_3)_3\cdot 6H_2O$ (177 mg, 0.5 mmol), and L-abaH (103 mg, 1 mmol) in MeOH (30 mL) was added NEt_3 (2 mmol). The resulting pale-green solution was left to stir for 25 min, during which time the solution turned green-purple. The solution was consequently filtered and allowed to slowly evaporate. Pink crystals of **5** formed over 2 days in ∼45% yield. Anal. Calcd (found) for **5**: C, 22.59 (22.46); H, 3.79 (3.53); N, 11.52 (11.64).

Physical Methods. Elemental analyses (C, H, N) were performed by the University of Ioannina microanalysis service. IR spectra (4000−450 cm^{-1}) were recorded as KBr pellets on a Jasco FT/IR-410 spectrophotometer. Variable-temperature, solid-state direct-current (dc) magnetic susceptibility data down to 2.0 K were collected on a Quantum Design MPMS-XL SQUID magnetometer equipped with a 5 T dc magnet at The University of Crete. Diamagnetic corrections were applied to the observed paramagnetic susceptibilities using Pascal's constants.

X-ray Crystallography and Structure Solution. Diffraction data for complexes **1**, **3**, and **4** were collected on an Xcalibur PX diffractometer with CCD Onyx and for **2** and **5** on a KM4 diffractometer with a CCD sapphire camera and Mo Kα radiation (λ = 0.710 73 Å). The crystal for **2** was slowly cooled from room temperature to 100 K, at which data collection was carried out. On the contrary, slow cooling of crystal **3** resulted in its twinning; thus, it was immediately placed at 100 K (supercooling). All structures were solved by direct methods and refined by full-matrix least-squares techniques on F^2 (*SHELX*).[5]

In the structure of **1**, one of the methanol molecules coordinated to a Ni atom was split into two positions because of disorder. Most of the anions were disordered over two positions as well. In the structure of **2**, one of the Ni atoms was modeled as disordered over two positions with occupation factors of 0.74 and 0.36. The nitrate anions were disordered over three and two sites for N15 and N16, respectively. All water molecules are disordered. The refinement of structure **3** was started by using the coordinates for heavy atoms of the isomorphous structure of **2**. Additional disorder was introduced to the complex cation (one La atom disordered over three positions and two Ni atoms over two positions, each). The nitrate anions were disordered over two positions. The water molecules showed behavior similar to that in the structure of **2**. In the structure of **4**, two of four coordinated L-aba ligands show disorder (terminal ethyl groups occupy two positions). One of the coordination sites of Ni3 consists of water (50%) and ethanol (50%) molecules. In the structure of **5**, the terminal groups of three coordinated L-aba ligands were refined as disordered over two positions, each.

Data collection parameters and structure solution and refinement details are listed in Table 1. Full details for **1**−**5** can be found in the CIF files provided in the Supporting Information.

RESULTS AND DISCUSSION

Synthesis. The reaction between $Ni(NO_3)_2\cdot 6H_2O$, $La(NO_3)_3\cdot 6H_2O$, and aibH in the absence of a base in MeOH gives complex **1**, which was crystallographically identified as **1**·3.05MeOH. To our initial surprise, the complex contains only Ni^{II} ions, despite the fact that La^{III} ions were added in the reaction "blend" in a 2:1 (Ni^{II}/La^{III}) ratio. Furthermore, repeating the same reaction in the absence of the Ln^{III} ions did not lead to any crystalline material. Therefore, we repeated the synthetic procedure with decreased ratios of Ni^{II}/La^{III} as a means to "force" the Ln centers into the reaction product. Nevertheless, our attempts were not successful even at Ni^{II}/La^{III} ratios as low as 1:3. With the identity of complex **1** established, we repeated the synthetic procedure by adding a base, NEt_3, to our reaction mixture while keeping all other reaction conditions unchanged (e.g., reaction time, concentrations, etc.). This was done as a means of creating OR^-/O^{2-} groups that would favor the binding of the oxophilic Ln ions. Indeed, the result was the isolation of complex **2**, in which both Ni^{II} and La^{III} centers are present, albeit with no OR^-/O^{2-} groups present. A possible explanation may lie in the ratios employed. The ratio of Ni^{II}/aib^- in complex **1** is 2:3 (considering the deprotonated carboxylic group of the ligands present), while in **2**, this ratio has decreased to 1:2. The addition of a base increased the amount of aib^-, leading to a lower Ni/aib ratio, resulting in the presence of more O-containing ligands, and therefore to encapsulation of the oxophilic Ln^{III} ion. This assumption is further supported by the fact that in both **1** and **2** the ligand is found in the same binding mode (vide infra). With the identity of complex **2** established, the next obvious step was the synthesis and characterization of an analogous Ni_6Ln complex in which the Ln center would be both paramagnetic and magnetically anisotropic. Therefore, we repeated the synthesis of **2** but with the use of $Pr(NO_3)_3\cdot 6H_2O$ as the lanthanide source, and complex **3** was formed. Complexes **2** and **3** are isostructural and only differ in the nature of the central lanthanide. Similar $[Ni_6Ln]$ complexes have been isolated and reported in the past with the use of naturally occurring amino acids (vide infra). Having isolated complexes **1**−**3** with the use of aibH, we then

dx.doi.org/10.1021/ic2004744 |*Inorg. Chem.* 2011, 50, 5175–5185

Table 1. Crystallographic Data for Complexes 1−5

	1·3.05MeOH	**2**·5.5H_2O	**3**·5.5H_2O	**4**·0.4EtOH·0.3H_2O	**5**
formula[a]	$C_{32.05}H_{83.20}N_{11}Ni_4O_{35.05}$	$C_{48}H_{107}LaN_{15}Ni_6O_{38.5}$	$C_{48}H_{107}N_{15}Ni_6O_{38.50}Pr$	$C_{26.80}H_{57}N_4Ni_5O_{20.70}$	$C_{48}H_{96}LaN_{12}Ni_6O_{24}\cdot La_2N_9O_{27}$
M_w	1418.54	2001.66	2003.66	1060.11	2552.45
cryst syst	triclinic	orthorhombic	orthorhombic	orthorhombic	cubic
space group	$P\bar{1}$	*Pnnm*	*Pnnm*	*I*222	$P2_13$
a/Å	11.950(4)	16.557(5)	16.373 (7)	13.172 (6)	21.510 (7)
b/Å	12.369(4)	17.905(5)	17.206 (8)	17.242 (8)	
c/Å	21.992(6)	14.130(4)	13.912 (4)	22.112 (10)	
α/deg	91.86(3)				
β/deg	101.19(3)				
γ/deg	103.07(3)				
V/Å^3	3096.3(17)	4189(2)	3919(3)	5022(4)	9952(10)
Z	2	2	2	4	4
T/K	100(2)	298(2)	100	100	110
λ[b]/Å	0.710 73	0.710 73	0.710 73	0.710 73	0.710 73
D_c/g cm^{-3}	1.522	1.587	1.698	1.402	1.704
μ(Mo Kα)/ mm^{-1}	1.30	1.91	2.12	1.91	2.46
measd/indep (R_{int}) reflns	32 935/16 778 (0.022)	51 641/5256 (0.061)	18 237/4641 (0.025)	14 198/5484 (0.077)	130 979/13 567 (0.057)
obsd reflns [$I > 2\sigma(I)$]	12 337	4458	3786	2700	10 145
wR2[c,d]	0.108	0.131	0.103	0.189	0.136
R1[d,e]	0.038	0.042	0.039	0.062	0.047
GOF on F^2	1.062	1.05	1.10	1.04	1.08
$\Delta\rho_{max,min}$/e Å^{-3}	1.04, −0.90	1.13, −1.03	1.34, −1.51	1.33, −0.81	2.49, −1.09

[a] Including solvate molecules, Mo Kα radiation, and a graphite monochromator. [c] wR2 = $[\Sigma w(|F_o^2| - |F_c^2|)^2/\Sigma w|F_o^2|^2]^{1/2}$. [d] For observed data. [e] R1 = $\Sigma||F_o| - |F_c||/\Sigma|F_o|$.

modified the amino acid in order to investigate how this would affect the identity of the product. Therefore, we turned our attention to L-abaH, an isomer of 2-aminoisobutyric acid. Even though the two ligands employed in our work are structural isomers, their differences could quite easily affect the structures and/or magnetic properties of the products. Initial attempts to isolate any crystalline material with the use of $Ni(NO_3)_2\cdot 6H_2O$ as the source of Ni^{II} were not fruitful, and therefore we employed $Ni(OAc)_2\cdot 2H_2O$. Indeed, the reaction between $Ni(OAc)_2\cdot 4H_2O$, $La(NO_3)_3\cdot 6H_2O$, and L-abaH in alcoholic solvents in the absence of a base led to the formation of the homometallic Ni^{II} pentanuclear (vs tetranuclear in the case of aibH) complex **4**, in which the Ln ions do not participate in the reaction product as in the case of **1**. We tried to repeat the synthesis of **4** without adding La^{III} in the reaction mixture, but all of our attempts were unsuccessful. In order to verify our initial hypothesis that it was the added base that was responsible for lanthanide encapsulation, we repeated the synthesis of **4** in the presence of NEt_3. The result was the formation of **5**, which can be regarded as the "L-abaH analogue" of complexes **2** and **3**. Interestingly, the counterion in the case of complex **5** is the lanthanide dimer, $[La_2(NO_3)_9]^{3-}$. It is noteworthy that, although L-abaH affects the identity of the homometallic Ni^{II} product, it does not affect the identity of the heterometallic complex. Also, despite the structural similarity of aibH and L-abaH, the ligands do not adopt the same binding modes (Scheme 1, vide infra).

The coordination chemistry of 2-aminobutyric acid has scarcely been investigated, with the only metal complexes reported so far being a europium(III) monomer and four copper(II) monomers.[6] On the other hand, the coordination chemistry of

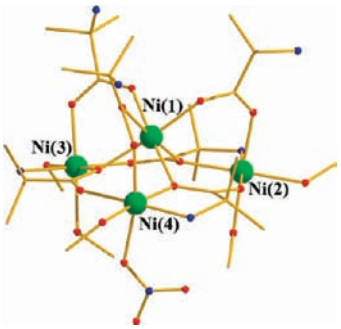

Figure 1. Molecular structure of the cation of complex **1**. Color code: Ni^{II}, green; O, red; N, blue; C, gold.

2-aminoisobutyric acid has been explored more extensively. Yet again, most of the complexes isolated are monomers or dimers (i.e., in the case of lanthanides),[7] with the only exceptions being a beautiful impressive $[Cu_{24}Gd_6]$ complex[8] and a $[Zn_3]$ complex.[9]

Description of the Structures. The structure of complex **1** is shown in Figure 1, with select bond lengths and angles given in Table 2. The central core of **1** describes a $[Ni_4(aib)_3(aibH)_3]^{5+}$ trigonal pyramid, in which the basal metal centers occupy the corners of an isosceles triangle (Ni3···Ni2 = Ni2···Ni4, ∼5.4 Å; Ni3···Ni4, ∼5.3 Å), with the edges of the triangle consisting of aib^- ligands. The height of the pyramid is ∼1.45 Å. The aib^- ligands coordinate as shown in Scheme 1 to produce the $[Ni_4(aib)_3(aibH)_3]^{5+}$ magnetic core in which the peripheral metal atoms are connected to each other via three $\eta^2{:}\eta^1{:}\eta^1{:}\mu_3$-$aib^-$ ligands, which also bond to the central Ni center via three

dx.doi.org/10.1021/ic2004744 |*Inorg. Chem.* 2011, 50, 5175–5185

Table 2. Select Interatomic Distances (Å) and Angles (deg) for 1·3.05MeOH

Ni1−O11	2.0345(18)	Ni2−O26	2.0192(17)	Ni3−O15	2.0295(15)
Ni1−O12	2.0515(16)	Ni2−O21	2.0224(18)	Ni3−N15	2.0573(19)
Ni1−O13	2.0547(17)	Ni2−O14	2.0386(16)	Ni4−O25	2.0334(17)
Ni1−O15	2.0551(17)	Ni2−N14	2.063(2)	Ni4−O16	2.0405(17)
Ni1−O16	2.0624(15)	Ni3−O22	2.0202(16)	Ni4−N16	2.045(2)
Ni1−O14	2.0749(16)	Ni3−O24	2.0224(16)	Ni4−O23	2.051(2)
				Ni4−O114	2.132(2)
O11−Ni1−O12	87.50(7)	O13−Ni1−O14	175.14(6)	O22−Ni3−N15	89.95(7)
O11−Ni1−O13	84.34(7)	O15−Ni1−O14	92.21(7)	O24−Ni3−N15	178.99(6)
O12−Ni1−O13	87.42(7)	O16−Ni1−O14	88.52(6)	O15−Ni3−N15	81.71(7)
O11−Ni1−O15	173.41(6)	O26−Ni2−O21	89.98(7)	O25−Ni4−O16	99.33(7)
O12−Ni1−O15	92.29(6)	O26−Ni2−O14	97.01(6)	O25−Ni4−N16	179.01(8)
O13−Ni1−O15	89.08(7)	O21−Ni2−O14	93.32(7)	O16−Ni4−N16	81.51(8)
O11−Ni1−O16	90.83(7)	O26−Ni2−N14	177.04(8)	O25−Ni4−O23	88.27(7)
O12−Ni1−O16	175.87(6)	O21−Ni2−N14	87.84(9)	O16−Ni4−O23	93.41(7)
O13−Ni1−O16	96.17(7)	O14−Ni2−N14	81.12(7)	N16−Ni4−O23	92.21(9)
O15−Ni1−O16	89.80(6)	O22−Ni3−O24	89.78(7)	O25−Ni4−O114	81.28(7)
O11−Ni1−O14	94.36(7)	O22−Ni3−O15	93.62(7)	O16−Ni4−O114	92.44(7)
O12−Ni1−O14	87.85(6)	O24−Ni3−O15	99.28(7)	N16−Ni4−O114	98.18(9)
				O23−Ni4−O114	168.73(7)

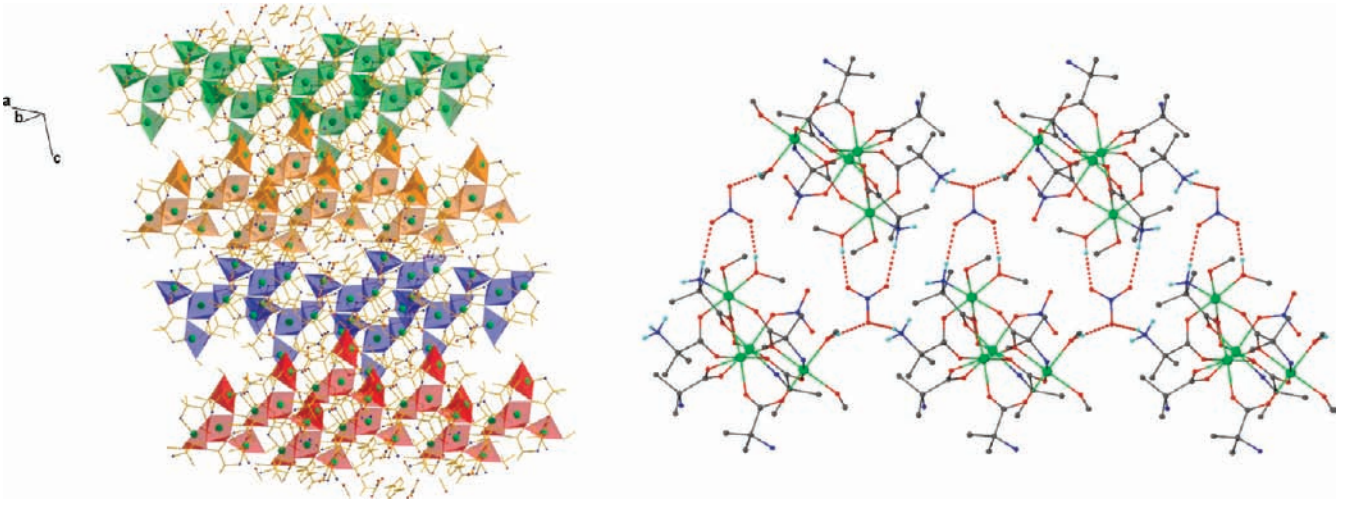

Figure 2. Crystal packing (left) and hydrogen bonding (right) in **1**. The differently colored nickel(II) polyhedra indicate molecules belonging to neighboring sheets. Color code: same as that in Figure 1.

monatomic $O_{carboxylate}$ bridges. The bonding of the peripheral Ni atoms to the central Ni3 ion is further supported by three additional *syn,syn*-η^1:η^1:μ_2-aibH ligands in their zwitterionic form. The coordination spheres for the Ni atoms are completed by four MeOH molecules and one NO_3^- anion, which is terminally bonded to Ni4. Each Ni center is six-coordinate, adopting a distorted octahedral geometry. Alternatively, the core of the structure can be described as a $[Ni_4(OR)_3]^{5+}$ "star", in which the central Ni atom (Ni1) is connected via three monatomic bridges (from three η^2:η^1:η^1: μ_3-aib$^-$ ligands) with the three peripheral Ni atoms. A detailed CCDC search reveals a total of 397 Ni^{II}_4 complexes, with the vast majority describing $[Ni_4(OR)_4]^{n+}$ cubanes, distorted cubanes, cubes (i.e., cubanes with diatomic bridges present), defective double cubanes, $[Ni_4(OR)_6]^{n+}$ squares, rectangles, "dimer-of-dimers", and linear topologies. From all ~400 structures, there is only one report of a similar Ni^{II}_4 star, whose magnetic ground state has not been reported.[10]

In the crystal lattice, the molecules stack upon each other in a "head-to-head" fashion, forming sheets with the solvent molecules and the nitrate counterions occupying the space within these sheets (Figure 2, left). In addition, the $[Ni_4]$ molecules and the non-disordered nitrate form a one-dimensional tape along the *b* axis. The rest of the disordered solvates as well as the disordered NO_3^- participate in the hydrogen bonding connecting the tapes to the three dimensions, but because of their highly disordered nature, analysis of the hydrogen-bonded network is not possible (Figure 2, right).

The structures of complexes **2**, **3**, and **5** are shown in Figures 3 and 4, with select bond lengths and angles given in Tables 3, 4, and 6. Complexes **2**, **3**, and **5** display very similar structures, and

dx.doi.org/10.1021/ic2004744 |*Inorg. Chem.* 2011, 50, 5175–5185

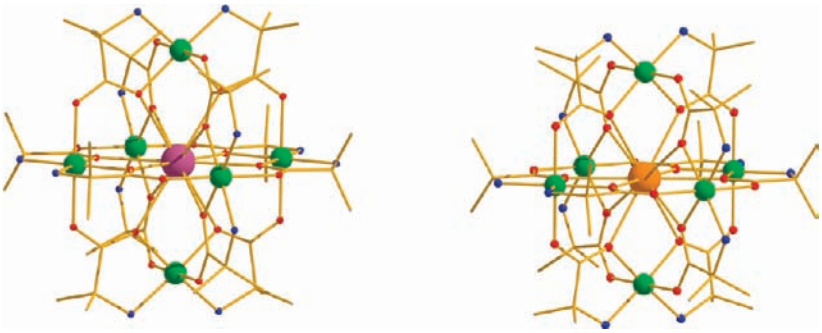

Figure 3. Molecular structures of the cations of complexes **2** (left) and **3** (right). Color code: Ni^{II}, green; La^{III}, purple; Pr^{III}, orange; O, red; N, blue; C, gold.

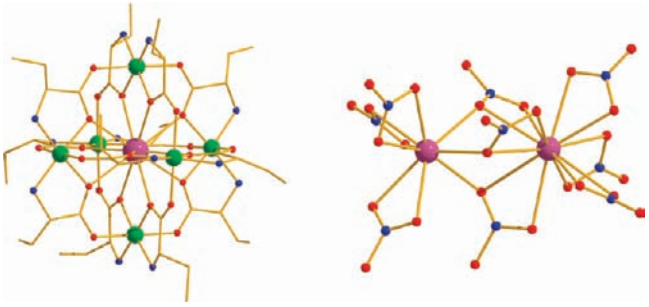

Figure 4. Molecular structure of complex **5**. Color code: Ni^{II}, green; La^{III}, purple; O, red; N, blue; C, gold.

so for the sake of brevity, we provide a generic description, highlighting individual differences. Their metallic core consists of a Ni^{II}_6 octahedron, which encapsulates one Ln^{III} ion. The encapsulation of the Ln^{III} ion occurs via 12 deprotonated aib$^-$ (L-aba$^-$ in the case of **5**) ligands, which each bonds to the central Ln ion via one monatomic O_{CO_2} bridge, providing Ln^{III} with an icosahedral coordination sphere (Figure 5, left). The Ln^{III} ion is held captive within the cavity of three macrocycles, which are assembled perpendicular to each other, with the threading points being the Ni^{II} centers, forming a cryptand-like molecule (Figure 5, right). The 12 aib$^-$ (L-aba$^-$ for **5**) ligands all bond in a $\eta^2{:}\eta^1{:}\eta^1{:}\mu_3$ fashion, and each Ni center is six-coordinate, adopting a distorted octahedral geometry. For **5**, the structure of the counteranion $[La^{III}_2(NO_3)_9]^{3-}$ consists of two La^{III} ions at ~4 Å bridged by three $\eta^2{:}\eta^1{:}\mu$ NO_3^-. In addition, each La^{III} center "carries" three chelate nitrates. The closest $[Ni_6La]^{3+}\cdots[La_2(NO_3)_9]^{3-}$ distance is ~12 Å. For complexes **2** and **3** in the crystal, each $[Ni_6Ln]$ complex sits directly on top of another, creating a column of $[Ni_6Ln]$ molecules encapsulating the nitrates and the solvate molecules (Figure 6), while for complex **5**, the $[Ni_6La]$ and $[La_2]$ units assemble through multiple hydrogen bonds to form a three-dimensional framework that conforms to the **pcu**-$(4^{12}.6^3)$ net (Figure 7). In this arrangement, each $[Ni_6La]$ unit is connected to six $[La_2]$ units, and each $[La_2]$ moiety is connected to six $[Ni_6La]$ species. Therefore, the underlying net is uninodal, with two chemically different nodes of the same connectivity.

Complex **4** crystallizes in the chiral (orthorhombic) space group *I*222. Select bond lengths and angles are given in Table 5. Its metallic core consists of two corner-sharing, scalene $[Ni_3(\mu_3\text{-}OH)]^{4+}$ triangles (Ni1···Ni2, 2.85 Å; Ni2···Ni3, ~3.0 Å; Ni1···Ni3, 3.47 Å), with the edges of the triangles consisting of L-aba$^-$ and acetate ligands (Figure 8). Alternatively, the structure may be considered to be square-based pyramidal, in which the central apical Ni^{II} ion, Ni1, is located at ~1.3 Å above the mean plane defined by the remaining four Ni centers. The L-aba$^-$ ligands coordinate in two ways: two of them in a $\eta^2{:}\eta^1{:}\eta^1{:}\mu_3$ fashion, responsible for the intertriangular linkage, and the remaining two in a $\eta^2{:}\eta^1{:}\mu$ manner with one "free" carboxylate oxygen, responsible for the intratriangular stability. Furthermore, there are four $\eta^1{:}\eta^1{:}\mu$ acetates bridging Ni centers belonging to the same triangle. In the crystal lattice, the molecules of **4** form a two-dimensional hydrogen-bonded square grid parallel to the *ab* plane (Figure 8, right). A thorough CCDC search revealed 81 discrete $[Ni_5]$ clusters reported so far, with complex **4** being only the second chiral Ni^{II}_5 cluster.[11]

dc Magnetic Susceptibility Studies. Variable-temperature dc magnetic susceptibility data were collected for all complexes in the temperature range 5.0−300 K under an applied field of 0.1 T. These are plotted as $\chi_M T$ versus T in Figure 9. For **1**, the room temperature $\chi_M T$ value of 4.34 cm^3 K mol^{-1} is slightly lower than the expected value of 4.41 cm^3 K mol^{-1} for four noninteracting Ni^{II} ions (with $g = 2.1$). Upon cooling, the value of $\chi_M T$ remains almost constant until ~50 K, below which it increases to a maximum value of 5.03 cm^3 K mol^{-1} at 6.5 K and then decreases to 4.97 cm^3 K mol^{-1} at 5 K. This behavior is consistent with the presence of both antiferromagnetic and ferromagnetic interactions between the metal centers, with the low-temperature value indicating an $S \approx 2$ spin ground state. We were able to successfully simulate the magnetic susceptibility data using the 3*J* model of Figure 10 and Hamiltonian equation (1), which assumes the following exchange interactions: one exchange (J_1) between the peripheral Ni^{II} ions and the central Ni^{II} ion (mediated by one monatomic and one *syn,syn*-$\eta^1{:}\eta^1{:}\mu_2$-carboxylate bridge) and two *J*'s (J_2 and J_3) between the Ni pairs located on the isosceles triangular base of the trigonal pyramid: J_2 between Ni3···Ni2 and Ni2···Ni4 and J_3 between Ni3···Ni4, all mediated by one $\eta^2{:}\eta^1{:}\eta^1{:}\mu_3$-carboxylate bridge. Using the program *MAGPACK*[12] and employing the Hamiltonian in eq 1

$$\hat{H} = -2J_1(\hat{S}_1\cdot\hat{S}_2 + \hat{S}_1\cdot\hat{S}_3 + \hat{S}_1\cdot\hat{S}_4) - 2J_2(\hat{S}_2\cdot\hat{S}_3 + \hat{S}_2\cdot\hat{S}_4) - 2J_3(\hat{S}_3\cdot\hat{S}_4) \quad (1)$$

afforded the parameters J_1 = 3.15 cm^{-1}, J_2 = −2.05 cm^{-1}, J_3 = −0.95 cm^{-1}, and g = 2.08. The ground state of **1** was found to be S = 2, with the first excited state (S = 3) located only 1.2 cm^{-1} above. The ferromagnetic nature of J_1 may be attributed

dx.doi.org/10.1021/ic2004744 |*Inorg. Chem.* 2011, 50, 5175–5185

Table 3. Select Interatomic Distances (Å) and Angles (deg) for $2 \cdot 5.5H_2O$[a]

La−O11	2.719(2)	Ni1−O21	2.057(3)	Ni3−O14	1.971(6)
La−O13	2.735(3)	Ni2−O11	2.029(2)	Ni3−N14	2.006(6)
La−O14	2.746(3)	Ni2−N11	2.049(3)	Ni3−O22	2.080(2)
La−O12	2.746(2)	Ni2−O23^{i}	2.062(3)	Ni3−O13	2.081(5)
Ni1−O12	2.035(2)	Ni2−O24	2.063(3)	Ni3−N13	2.109(7)
Ni1−N12	2.042(3)				
O11^{ii}−La−O11	114.66(9)	O13−La−O14	64.86(9)	O11−La−O12	62.95(6)
O11−La−O13^{i}	63.36(6)	O12−La−O12^{iii}	114.17(9)	O13−La−O12	62.69(5)
O11−La−O14	62.96(6)	O11^{ii}−La−O12	63.16(6)	O14−La−O12	62.72(5)

[a] Symmetry codes: (i) $-x+1, -y+1, -z+1$; (ii) $-x+1, -y+1, z$; (iii) $x, y, -z+1$; (iv) $-x+1, -y+2, z$.

Table 4. Select Interatomic Distances (Å) and Angles (deg) for $3\ 5.5H_2O$[a]

Pr−O11	2.706(3)	Ni1−O12	2.030(3)	Ni2−N11	2.049(4)
Pr−O12	2.710(3)	Ni1−O21	2.050(3)	Ni2−O24	2.060(4)
Pr−O13	2.703(4)	Ni2−O11	2.024(3)	Ni3−O13	2.036(4)
Pr−O14	2.734(4)	Ni2−O23^{i}	2.030(4)	Ni3−N13	2.058(6)
Ni1−N12	2.041 (4)				
O13−Pr−O11	116.78(9)	O11^{ii}−Pr−O12	63.35(8)	O12−Pr−O12^{ii}	65.81(12)
O11−Pr−O11^{iii}	65.33(12)	O11−Pr−O12	62.76(8)	O14−Pr−O12	62.60(6)
O13−Pr−O12	62.87(6)	O12^{iii}−Pr−O12	114.19(12)		

[a] Symmetry codes: (i) $-x+1, -y+1, -z+1$; (ii) $-x+1, -y+1, z$; (iii) $x, y, -z+1$.

Table 5. Select Interatomic Distances (Å) and Angles (deg) for $4 \cdot 0.4EtOH \cdot 0.3H_2O$[a]

Ni1−O22	2.025(8)	Ni2−O12	2.080(8)	Ni3−N14	2.066(10)
Ni1−O1	2.060(7)	Ni2−O14	2.110(7)	Ni3−O21^{i}	2.107(7)
Ni1−O11	2.068(7)	Ni3−O1	2.030(7)	Ni3−O13	2.114(6)
Ni2−O11	2.025(6)	Ni2−O23	2.033(6)	Ni3−O14	2.039(7)
Ni2−N11	2.075(8)	Ni2−O1	2.059(7)	Ni3−O15	2.047(8)
O22^{i}−Ni1−O22	93.1(5)	O11−Ni2−O23	179.2(4)	O1−Ni3−O13	89.6(3)
O22^{i}−Ni1−O1^{i}	90.8(3)	O11−Ni2−O1	83.7(2)	O14−Ni3−O13	90.3(3)
O22−Ni1−O1^{i}	93.8(3)	O23−Ni2−O1	96.7(3)	O15−Ni3−O13	86.2(3)
O22^{i}−Ni1−O1	93.8(3)	O11−Ni2−N11	81.0(3)	N14−Ni3−O13	88.6(4)
O22−Ni1−O1	90.8(3)	O23−Ni2−N11	98.6(3)	O21^{i}−Ni3−O13	170.3(3)
O1^{i}−Ni1−O1	173.3(5)	O1−Ni2−N11	163.7(3)	Ni3−O1−Ni2	95.4(3)
O22^{i}−Ni1−O11	175.4(3)	O11−Ni2−O12	89.6(3)	Ni3−O1−Ni1	126.9(4)
O22−Ni1−O11	89.9(3)	O23−Ni2−O12	91.1(3)	Ni2−O1−Ni1	94.0(3)
O1^{i}−Ni1−O11	92.4(3)	O1−Ni2−O12	92.4(3)	O15−Ni3−N14	98.6(3)
O1−Ni1−O11	82.7(3)	N11−Ni2−O12	93.0(3)	O1−Ni3−O21^{i}	98.8(3)
O22^{i}−Ni1−O11^{i}	89.9(3)	O11−Ni2−O14	91.9(3)	O14−Ni3−O21^{i}	95.2(3)
O22−Ni1−O11^{i}	175.4(3)	O23−Ni2−O14	87.5(3)	O15−Ni3−O21^{i}	88.2(3)
O1^{i}−Ni1−O11^{i}	82.7(3)	O1−Ni2−O14	81.3(3)	N14−Ni3−O21^{i}	84.5(3)
O1−Ni1−O11^{i}	92.4(3)	N11−Ni2−O14	93.6(3)	O14−Ni3−O15	176.4(3)
O11−Ni1−O11^{i}	87.2(4)	O12−Ni2−O14	173.4(3)	O1−Ni3−N14	164.4(3)
O1−Ni3−O14	83.8(3)	O1−Ni3−O15	96.8(3)	O14−Ni3−N14	80.7(3)

[a] Symmetry code: (i) $-x+1, -y+1, z$.

to countercomplementarity effects between the monatomic carboxylate bridge and the *syn,syn*-η^1:η^1:μ_2-bridging carboxylate.[13]

Complexes **2** and **5** ([Ni_6La] analogues) display similar magnetic behavior. For **2**, the room temperature $\chi_M T$ value of 7.21 $cm^3\ K\ mol^{-1}$ is slightly lower than the expected value of 7.26 $cm^3\ K\ mol^{-1}$ for six noninteracting Ni^{II} ions (with $g = 2.2$). Upon cooling, the value of $\chi_M T$ remains almost constant until ~80 K, below which it decreases to a minimum value of 4.76 $cm^3\ K\ mol^{-1}$ at 5 K. This behavior is consistent with the presence of dominant antiferromagnetic interactions between the metal

dx.doi.org/10.1021/ic2004744 |*Inorg. Chem.* 2011, 50, 5175–5185

Table 6. Select Interatomic Distances (Å) and Angles (deg) for 5[a]

La1−O13	2.720(3)	Ni1−O12^{ii}	2.048(3)	Ni2−N13	2.048(4)
La1−O11	2.722(3)	Ni1−N12^{ii}	2.048(4)	Ni2−O14^{i}	2.050(3)
La1−O14	2.723(3)	Ni1−O22^{i}	2.053(3)	Ni2−N14^{i}	2.057(4)
La1−O12	2.736(3)	Ni1−O24^{i}	2.063(3)	Ni2−O21^{i}	2.072(3)
Ni1−O11	2.035(3)	Ni2−O13	2.042(3)	Ni2−O23^{ii}	2.075(4)
Ni1−N11	2.040(4)				
O13−La1−O13^{i}	62.46(10)	O13^{ii}−La1−O12	179.13(8)	O11−La1−O14^{i}	63.48(9)
O13−La1−O11^{i}	64.06(9)	O11^{i}−La1−O12	65.38(8)	O14^{i}−La1−O14^{ii}	117.26(3)
O13−La1−O11	118.10(9)	O11−La1−O12	116.77(8)	O13−La1−O14	117.11(9)
O13^{i}−La1−O11	114.58(8)	O11^{ii}−La1−O12	61.42(8)	O13^{i}−La1−O14	63.09(8)
O11^{i}−La1−O11	116.58(4)	O14−La1−O12	113.95(8)	O11^{i}−La1−O14	178.77(9)
O13−La1−O14^{i}	66.10(9)	O12^{i}−La1−O12	63.83(9)	O11−La1−O14	62.65(8)
O13−La1−O12	116.96(8)	O14^{i}−La1−O12	117.39(8)	O14^{i}−La1−O14	117.26(3)
O13^{i}−La1−O12	116.74(8)	O14^{ii}−La1−O12	62.06(8)		

[a] Symmetry codes: (i) *y*, *z*, *x*; (ii) *z*, *x*, *y*.

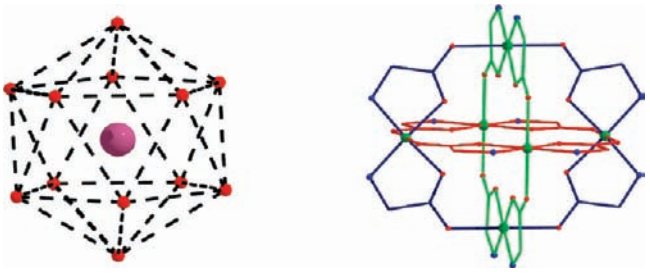

Figure 5. Lanthanide(III) icosahedron in **2**, **3**, and **5** (left). Cryptand-like molecule responsible for encapsulating the Ln^{III} center in **2** and **3** (right). Color code: Ni^{II}, green; Ln^{III}, purple; O, red; N, blue; C, gold.

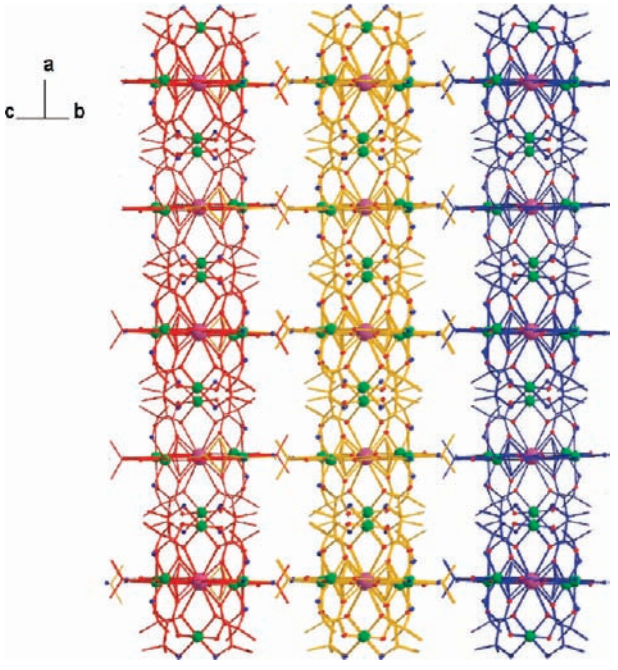

Figure 6. Column-like packing of **2** in the crystal lattice. Molecules of the same color belong to the same column. The noncoordinate nitrates and solvate molecules are omitted for clarity.

centers. We were able to successfully simulate the magnetic susceptibility data using a model that assumes only one *J* between the Ni^{II} ions (Figure 10, center). Using the program *MAGPACK* and employing the Hamiltonian of eq 2

$$\hat{H} = -2J_1(\hat{S}_1\cdot\hat{S}_2 + \hat{S}_1\cdot\hat{S}_3 + \hat{S}_1\cdot\hat{S}_4 + \hat{S}_1\cdot\hat{S}_5 + \hat{S}_2\cdot\hat{S}_3 + \hat{S}_2\cdot\hat{S}_4 + \hat{S}_2\cdot\hat{S}_5 + \hat{S}_2\cdot\hat{S}_6 + \hat{S}_3\cdot\hat{S}_4 + \hat{S}_3\cdot\hat{S}_5 + \hat{S}_3\cdot\hat{S}_6 + \hat{S}_4\cdot\hat{S}_5 + \hat{S}_4\cdot\hat{S}_6 + \hat{S}_5\cdot\hat{S}_6) \quad (2)$$

yielded the parameters $J = -0.4$ cm^{-1} and $g = 2.2$. The ground state of **2** was found to be $S = 0$, with the first excited state ($S = 1$) located only 0.8 cm^{-1} above. Similarly, for complex **5**, the parameters found were $J = -0.13$ cm^{-1} and $g = 2.18$, yielding a ground state of $S = 0$, with the first ($S = 1$) and second ($S = 2$) excited states located within 0.8 cm^{-1} above the ground state.

For complex **3**, the room temperature $\chi_M T$ of 8.15 cm^3 K mol^{-1} is close to the theoretical value of six noninteracting Ni^{II} ions with $S = 1$ and $g = 2.2$ and one Pr^{III} ($^3H_4$, $S = 1$, $L = 5$, $J = 4$, and $g_j = {}^4/_5$) of 8.85 cm^3 K mol^{-1}. Upon cooling, the $\chi_M T$ product decreases to a minimum value of 4.6 cm^3 K mol^{-1} at 5 K, suggesting the presence of dominant antiferromagnetic interactions and/or depopulation of the Stark sublevels of the Pr^{III} ion ($^3H_4$). The presence of the orbitally degenerate Pr^{III} ion precludes a fitting of the experimental data. Thus, it becomes apparent that all our [Ni_6Ln] complexes display dominant antiferromagnetic interactions, leading to small or even diamagnetic ground states (in the case of **2** and **5**) regardless of the ligand employed. Complexes **2**, **3**, and **5** join a small but growing family of structurally characterized [Ni_6Ln] clusters in which the Ln^{III} center is encapsulated within a Ni^{II}_6 octahedron (Table 7). Interestingly, not all of these complexes display the same magnetic behavior. It is noteworthy to compare and contrast the magnetic properties of **2** (and/or **5** and/or **6**) with **11** (and/or **14**). In each case, the metallic skeleton is identical with the diamagnetic Ln ion housed within a Ni_6 octahedron; i.e., the magnetic properties are solely based on the Ni···Ni exchange interactions. However, Zhang et al.[18] reported ferromagnetism in both **11** and **14**, while we and Aromi et al.[14] report antiferromagnetism with a diamagnetic ground state. This is also the case for complexes **3** and **13**, both of which contain the [Ni_6Pr] metal

dx.doi.org/10.1021/ic2004744 |*Inorg. Chem.* 2011, 50, 5175–5185

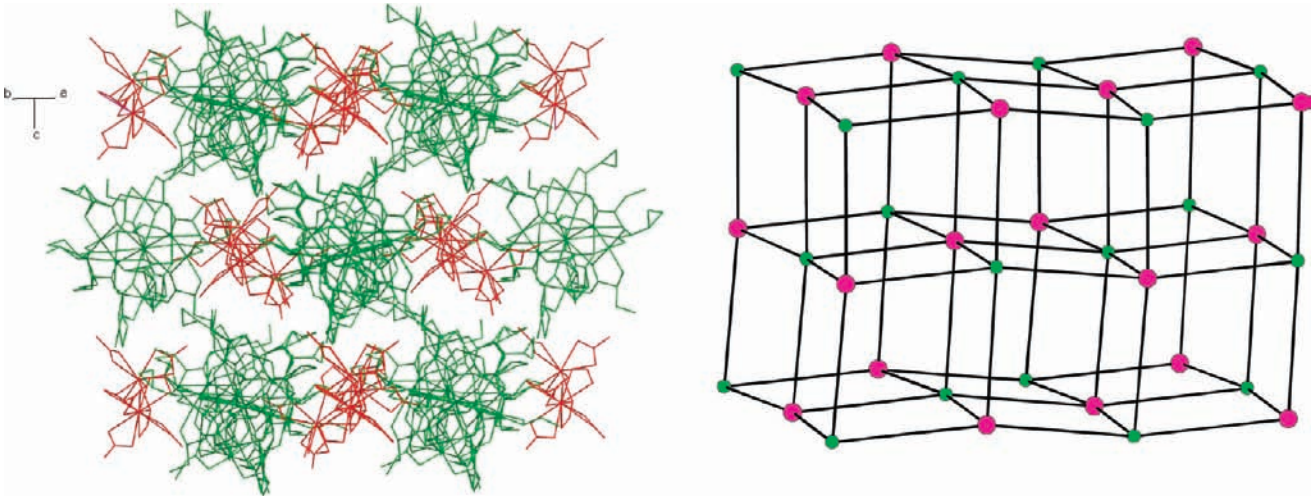

Figure 7. Packing of **5** in the crystal lattice (left) and the real pcu net (right). Color code: green, $[Ni_6La]^{3+}$ ions; red, $[Ln(NO_3)_9]^{3-}$ ions.

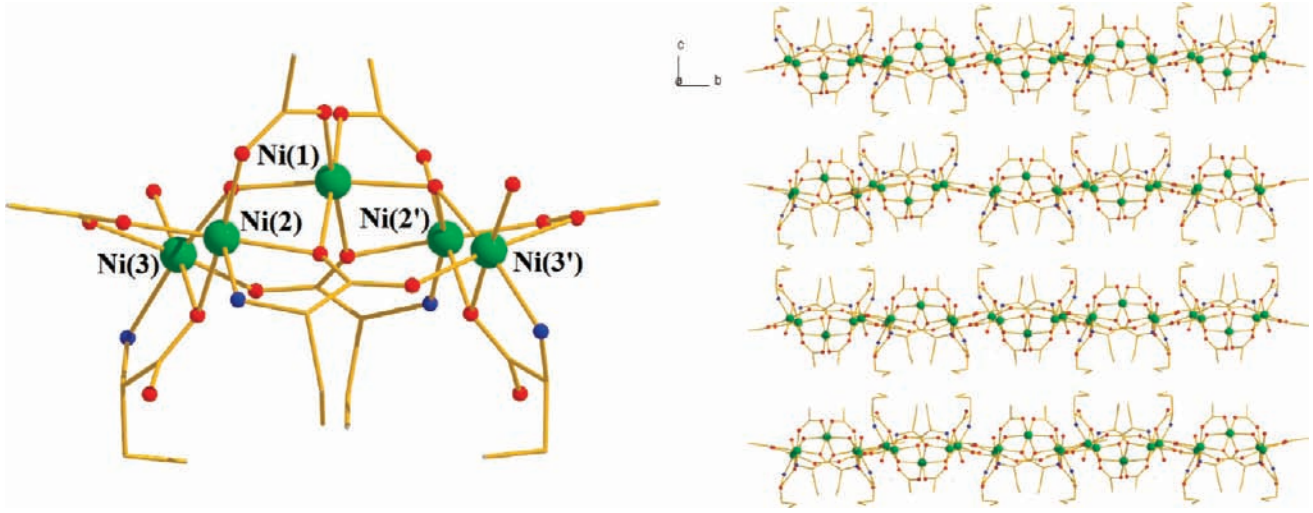

Figure 8. Molecular structure of complex **4** (left) and crystal packing in the lattice (right). Color code: same as that in Figure 1.

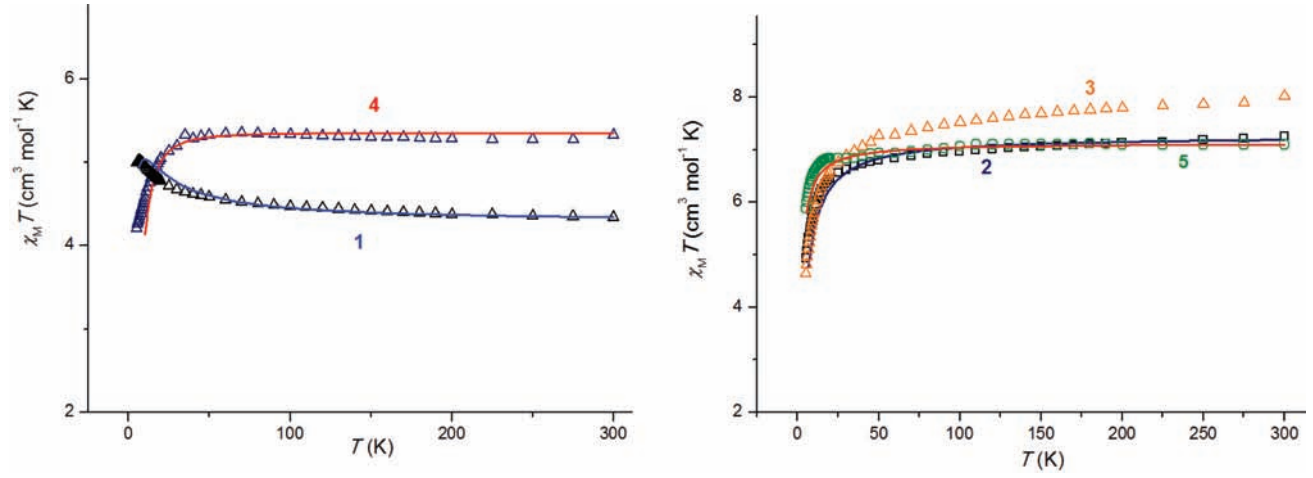

Figure 9. Plot of $\chi_M T$ vs T for complexes **1** (black triangles), **2** (black squares), **3** (orange triangles), **4** (blue triangles), and **5** (green circles). The solid lines represent a fit of the data in the temperature range 5−300 K (see the text for details).

dx.doi.org/10.1021/ic2004744 |*Inorg. Chem.* 2011, 50, 5175–5185

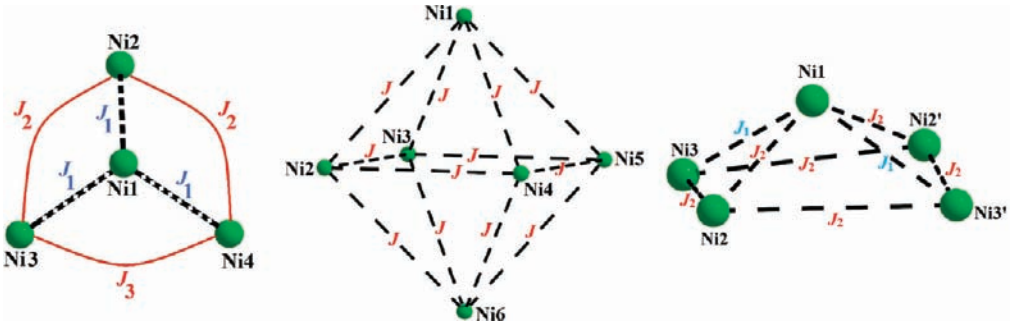

Figure 10. Exchange interaction models used for complexes **1** (left), **2** and **5**) (center), and **4** (right) (see the text for details).

Table 7. Formula and Spin Ground State for Structurally Characterized $[Ni_6Ln]$ Complexes

complex[a]	ground state, S	ref
$[Ni_6La(aib)_{12}](NO_3)_3 \cdot 5.5H_2O$ (**2**)	0	this work
$[Ni_6Pr(aib)_{12}](NO_3)_3$ (**3**)	N/A, antiferromagnetic behavior	this work
$[Ni_6La(\text{L-aba})_{12}][La_2(NO_3)_9]$ (**5**)	0	this work
$(NMe_4)[LaNi_6(pro)_{12}](ClO_4)_4$ (**6**)	0	14
$(NMe_4)[GdNi_6(pro)_{12}](ClO_4)_4$ (**7**)	$^{13}/_2$	14
$(NMe_4)[SmNi_6(pro)_{12}](ClO_4)_4$ (**8**)	N/A	15
$(NMe_4)[EuNi_6(pro)_{12}](ClO_4)_4$ (**9**)	N/A	16
$[Sm\{Ni(pro)_2\}_6][ClO_4]_3 \cdot 6MeOH$ (**10**)	N/A	17
$Na[LaNi_6(gly)_{12}](ClO_4)_4(H_2O)_{11}$ (**11**)	N/A, ferromagnetic behavior	18
$Na_5[LaNi_6(gly)_{12}](ClO_4)_8(H_2O)_{10}$ (**12**)	N/A	18
$Na[PrNi_6(gly)_{12}](ClO_4)_4(H_2O)_{11}$ (**13**)	N/A, ferromagnetic behavior	18
$[LaNi_6(gly)_{12}][Ni(im)(H_2O)_5](ClO_4)_5(H_2O)_5$ (**14**)	N/A, ferromagnetic behavior	18
$[LaNi_6(gly)_{12}][Ni(NCS)_3(H_2O)_3][Ni(NCS)_2(H_2O)_4](ClO_4)_2(H_2O)_6$ (**15**)	N/A	18
$[LaNi_6(ala)_{12}](ClO_4)_3\ (H_2O)_{15}$ (**16**)	N/A	18
$[LaNi_6(thr)_{12}](ClO_4)_3(H_2O)_{15}$ (**17**)	N/A	18
$\{La[Ni(L)]_6\}(ClO_4)_3$ (**18**)	N/A	19, 20
$\{Ce[Ni(L)]_6\}(ClO_4)_3$ (**19**)	N/A, antiferromagnetic behavior	19
$\{Pr[Ni(L)]_6\}(ClO_4)_3$ (**20**)	N/A	19
$\{Nd[Ni(L)]_6\}(ClO_4)_3$ (**21**)	N/A, antiferromagnetic behavior	19

[a] Abbreviations: aibH = 2-aminobutyric acid; L-abaH = L-2-aminobutyric acid; pro = proline; gly = glycine; ala = alanine; thr = threonine; L = tetradentate Schiff-base ligand.

core; complex **3** displays dominant antiferromagnetic exchange interactions, while **13** displays ferromagnetic behavior.[18] These findings strongly suggest that the magnetic behavior of such complexes depends on subtle geometric changes from one complex to another. This is further supported by the fact that, although both **2** and **5** are antiferromagnetically coupled with a diamagnetic ground state, **5** displays much weaker antiferromagnetic interactions than **2** (−0.13 vs −0.4 cm^{-1}), suggesting that switching from antiferromagnetic to ferromagnetic interaction is indeed plausible, especially because the magnetic interactions found in these clusters are very small in magnitude.

For complex **4**, the room temperature $\chi_M T$ of 5.32 $cm^3\ K\ mol^{-1}$ is very close to the theoretical value of 5.40 for five noninteracting Ni^{II} ions with $S = 1$ and $g = 2.08$. Upon cooling, the value of $\chi_M T$ remains almost constant until ∼50 K, below which it decreases to a minimum value of 4.16 $cm^3\ K\ mol^{-1}$ at 5 K, indicating the presence of a small spin ground state. Despite the presence of at least three different exchange interactions, we were able to successfully simulate the data, using the 2J model of Figure 10 (right) and Hamiltonian equation (3) assuming one J_1 between the central Ni1 ion and peripheral Ni3 and Ni3′ ions mediated by one μ_3-OH^- and one $\eta^2{:}\eta^1{:}\mu_3$-L-aba$^-$ carboxylate bridge and one J_2 between the Ni1−Ni2, Ni1−Ni2′, Ni2−Ni3, and Ni2′-Ni3′ pairs mediated by one μ_3-OH^-, one $\eta^2{:}\eta^1{:}\eta^1{:}\mu_3$-L-aba$^-$ carboxylate bridge, and one $\eta^1{:}\eta^1{:}\mu$-acetate bridge, as well as for the Ni2−Ni3′ and Ni3′-Ni2 pairs mediated by one $\eta^2{:}\eta^1{:}\mu_3$-L-aba$^-$ carboxylate bridge. Using the program *MAGPACK* and employing the Hamiltonian in eq 3

$$\hat{H} = -2J_1(\hat{S}_1 \cdot \hat{S}_3 + \hat{S}_1 \cdot \hat{S}_3 \cdot) - 2J_2(\hat{S}_1 \cdot \hat{S}_2 + \hat{S}_1 \cdot \hat{S}_2 \cdot + \hat{S}_2 \cdot \hat{S}_3 + \hat{S}_{2'} \cdot \hat{S}_{3'} + \hat{S}_2 \cdot \hat{S}_{3'} + \hat{S}_{2'} \cdot \hat{S}_3) \quad (3)$$

afforded the parameters $J_1 = 3.00\ cm^{-1}$, $J_2 = -1.00\ cm^{-1}$, and $g = 2.08$. The ground state of **4** was found to be $S = 1$, with the first excited state ($S = 2$) located only 4 cm^{-1} above. The ferromagnetic nature of J_1 may, as in the case of **1**, again be attributed to countercomplementarity effects between μ_3-OH^- and the $\eta^2{:}\eta^1{:}\mu_3$-L-aba$^-$ carboxylate bridge.

dx.doi.org/10.1021/ic2004744 |*Inorg. Chem.* 2011, 50, 5175–5185

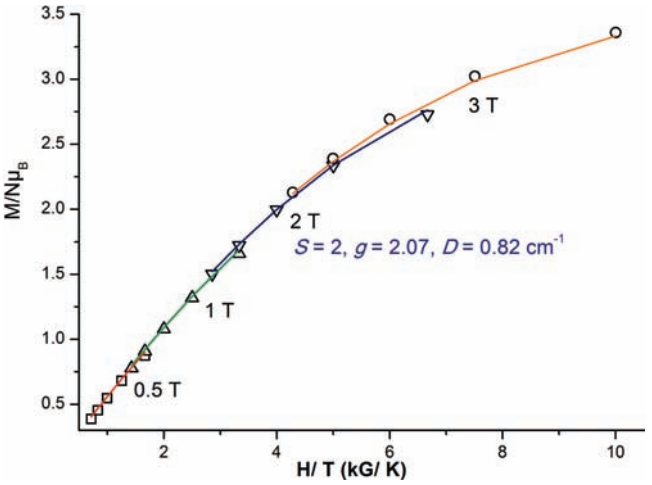

Figure 11. Plot of reduced magnetization ($M/N\mu_B$) versus H/T for **1** in the field and temperature ranges 0.5−3 T and 2−6 K. The solid lines correspond to the fit of the data.

In order to further determine the nature of the ground state of complex **1**, variable-temperature and variable-field dc magnetization data were collected in the ranges 2−6 K and 0.5−5 T, and these are plotted as reduced magnetization ($M/N\mu_B$) vs H/T in Figure 11. The 0.5−3 T data were fitted by a matrix diagonalization method to a model that assumes that only the ground state is populated, includes axial zero-field splitting ($D\hat{S}_z^2$) and the Zeeman interaction, and carries out a full powder average. The corresponding Hamiltonian is given by eq 4, where D is the axial anisotropy, μ_B is the Bohr magneton, μ_0 is the vacuum permeability, $\hat{S}_z$ is the easy-axis spin operator, and H is the applied field.

$$\hat{H} = D\hat{S}_z^2 + g\mu_B\mu_0\hat{S}\cdot H \quad (4)$$

The best fit gave $S = 2$, $g = 2.07$, and $D = +0.82$ cm^{-1}. Attempting to use data from higher fields (>3 T) resulted in a poor-quality fit, in agreement with the susceptibility data and the presence of low-lying excited states of larger S.

For complex **4**, no satisfactory fit of the data was possible because the magnetization rises almost linearly with the applied magnetic field, indicating the existence of small spin ground states with the presence of many low-lying excited states of larger multiplicity that become populated with increasing field. Low-lying excited states are a common problem in (large) polymetallic clusters, particularly when very weak exchange interactions are present, as is the case here.

CONCLUSIONS

The use of the artificial amino acids aibH and L-abaH in nickel(II) and nickel(II)/lanthanide(III) chemistry has led to the synthesis of five new homo- and heterometallic complexes. Furthermore, these synthetic systems are highly sensitive to the presence of a base that dictates the formation of either lanthanide-free nickel(II) clusters or heterometallic nickel(II)/lanthanide(III) complexes. In addition, the use of artificial amino acids in nickel(II) chemistry has led to the synthesis of polynuclear homometallic nickel(II) complexes (i.e., [Ni^{II}_4] and [Ni^{II}_5]), while the use of naturally occurring amino acids in nickel(II) chemistry has, so far, led to the synthesis of mononuclear complexes or catena-like structures.[21]

ASSOCIATED CONTENT

Supporting Information. Crystallographic data (CIF format). This material is available free of charge via the Internet at http://pubs.acs.org.

AUTHOR INFORMATION

Corresponding Author
*E-mail: komil@chemistry.uoc.gr.

ACKNOWLEDGMENT

C.J.M. thanks The University of Crete (ELKE Research Grant KA 3089) for funding.

REFERENCES

(1) Representative references and references cited therein: (a) Que, E. L.; Chang, C. J. *Chem. Soc. Rev.* **2010**, *39*, 51. (b) Fricker, S. P. *Chem. Soc. Rev.* **2006**, *6*, 524. (c) Murray, L. J.; Dincă, M.; Long, J. R. *Chem. Soc. Rev.* **2009**, *38*, 1294. (d) Manoli, M.; Collins, A.; Parsons, S.; Candini, A.; Evangelisti, M.; Brechin, E. K. *J. Am. Chem. Soc.* **2008**, *130*, 11129. (e) Bogani, L.; Wernsdorfer, W. *Nat. Mater.* **2008**, *7*, 179.

(2) (a) Gatteschi, D.; Sessoli, R. *Angew. Chem., Int. Ed.* **2003**, *42*, 268. (b) Christou, G.; Gatteschi, D.; Hendrickson, D. N.; Sessoli, R. *MRS Bull.* **2000**, *25*, 66.

(3) For reviews, see: (a) Aromi, G.; Brechin, E. K. *Struct. Bonding (Berlin)* **2006**, *122*, 1. (b) Christou, G.; Gatteschi, D.; Hendrickson, D. N.; Sessoli, R. *MRS Bull.* **2000**, *25*, 66. (c) Gatteschi, D.; Sessoli, R. *Angew. Chem., Int. Ed.* **2003**, *42*, 268. (d) Bircher, R.; Chaboussant, G.; Dobe, C.; Güdel, H. U.; Ochsenbein, S. T.; Sieber, A.; Waldman, O. *Adv. Funct. Mater.* **2006**, *16*, 209.

(4) (a) Sessoli, R.; Powell, A. K. *Coord. Chem. Rev.* **2009**, *253*, 2328. (b) Papatriantafyllopoulou, C.; Stamatatos, T.; Efthymiou, C. G.; Cunha-Silva, L.; Paz, F. A. A.; Perlepes, S. P.; Christou, G. *Inorg. Chem.* **2010**, *49*, 9743. (c) Efthymiou, C. G.; Stamatatos, T. C.; Papatriantafyllopoulou, C.; Tasiopoulos, A. J.; Wernsdorfer, W.; Perlepes, S. P.; Christou, G. *Inorg. Chem.* **2010**, *49*, 9739. (d) Mishra, A.; Wernsdorfer, W.; Parsons, S.; Christou, G.; Brechin, E. K. *Chem. Commun.* **2005**, 2086. (e) MereacreV.; Ako, A. M.; Clèrac, R.; Wernsdorfer, W.; Hewitt, I. J.; Anson, C. E.; Powell, A. K. *Chem.—Eur. J.* **2008**, *14*, 3577. (f) Abbas, G.; Lan, Y.; Mereacre, V.; Wernsdorfer, W.; Clèrac, R.; Buth, G.; Sougrati, M. T.; Grandjean, F.; Long, G. J.; Anson, C. E.; Powell, A. K. *Inorg. Chem.* **2009**, *48*, 9345. (g) Baskar, V.; Gopal, K.; Helliwell, M.; Tuna, F.; Wernsdorfer, W.; Winpenny, R. E. P. *Dalton Trans.* **2010**, *39*, 4747. (h) Chandrasekhar, V.; Pandian, B. M.; Boomishankar, R.; Steiner, A.; Vittal, J. J.; Houri, A.; Clèrac, R. *Inorg. Chem.* **2008**, *47*, 4918.

(5) Sheldrick, G. M. *Acta Crystallogr., Sect. A: Found. Crystallogr.* **2007**, *64*, 9484.

(6) (a) Liang, Y.; Wang, Z.; Jin, L. P.; Yan, C. *J. Mol. Struct.* **2002**, *616*, 231. (b) Fawcett, T. G.; Ushay, M.; Rose, J. P.; Lalancette, R. A.; Potenza, J. A.; Schugar, H. J. *Inorg. Chem.* **1979**, *18*, 327. (c) Dyakov, I. A.; Donu, S. V.; Chapurina, L. F. *Kristallografiya* **1998**, *43*, 656. (d) Levstein, P. R.; Calvo, R.; Castellano, E. E.; Piro, O. E.; Rivero, B. E. *Inorg. Chem.* **1990**, *29*, 3918.

(7) Aparna, K.; Krishnamurthy, S. S.; Nethaji, M.; Balaram, P. *Polyhedron* **1994**, *13*, 2993.

(8) Zhang, J.-J.; Hu, S.-M.; Xiang, S.-C.; Sheng, T.; Wu, X.-T.; Li, Y.-M. *Inorg. Chem.* **2006**, *45*, 7173.

(9) Katsoulakou, E.; Papaefstathiou, G. S.; Konidaris, K. F.; Pairas, G.; Raptopoulou, C.; Cordopatis, P.; Manessi-Zoupa, E. *Polyhedron* **2009**, *28*, 3387.

(10) Li, Y.; Xiang, S.; Sheng, T.; Zhang, J.; Hu, S.; Fu, R.; Huang, X.; Wu, X. *Inorg. Chem.* **2006**, *45*, 6577.
(11) Berry, J. F.; Cotton, F. A.; Lei, P.; Lu, T.; Murillo, C. A. *Inorg. Chem.* **2003**, *42*, 3534.
(12) (a) Borrás-Almenar, J. J.; Clemente-Juan, J. M.; Coronado, E.; Tsukerblat, B. S. *Inorg. Chem.* **1999**, *38*, 6081. (b) Borrás-Almenar, J. J.; Clemente-Juan, J. M.; Coronado, E.; Tsukerblat, B. S. *Comput. Chem.* **2001**, *22*, 985.
(13) (a) Palacios, M. A.; Mota, A. J.; Perea-Buceta, J. E.; White, F. J.; Brechin, E. K.; Colacio, E. *Inorg. Chem.* **2010**, *49*, 10156. (b) Mandal, S.; Balamurugan, V.; Lloret, F.; Mukherjee, R. *Inorg. Chem.* **2009**, *48*, 7544.
(14) Yukawa, Y.; Aromi, G.; Igarashi, S.; Ribas, J.; Zvyagin, S. A.; Krzystek, J. *Angew. Chem., Int. Ed.* **2005**, *44*, 1997.
(15) Igarashi, S.; Hoshino, Y.; Masuda, Y.; Yukawa, Y. *Inorg. Chem.* **2000**, *39*, 2509.
(16) Igarashi, S.; Yukawa, Y. *Chem. Lett.* **1999**, 1265.
(17) Yukawa, Y.; Igarashi, S.; Yamano, A.; Sato, S. *Chem. Commun.* **1997**, 711.
(18) Zhang, J.-J.; Xiang, S.-C.; Hu, S.-M.; Xia, S.-Q.; Fu, R.-B.; Wu, X.-T.; Li, Y.-M.; Zhang, H.-S. *Polyhedron* **2004**, *23*, 2265.
(19) Lin, X.; Doble, D. M. J.; Blake, A. J.; Harrison, A.; Wilson, C.; Schröder, M. *J. Am. Chem. Soc.* **2003**, *125*, 9477.
(20) Doble, D. M. J.; Benison, C. H.; Blake, A. J.; Fenske, D.; Jackson, M. S.; Kay, R. D.; Li, W. S.; Schröder, M. *Angew. Chem., Int. Ed.* **1999**, *38*, 1915.
(21) For example, see: (a) Muller, A.; Johannes, K. U.; Straube, M.; Krickemeyer, E.; Bogge, H. *Z. Anorg. Allg. Chem.* **1993**, *619*, 1037. (b) Cai, J.; Hu, X.; Bernal, I.; Ji, L.-N. *Polyhedron* **2002**, *21*, 817. (c) Fraser, K. A.; Harding, M. M. *J. Chem. Soc. A* **1967**, 415. (d) Battaglia, L. P.; Corradi, A. B.; Antolini, L.; Marcotrigiano, G.; Menabue, L.; Pellacani, G. C. *J. Am. Chem. Soc.* **1982**, *104*, 2407. (e) Antolini, L.; Menabue, L.; Pellacani, G. C.; Marcotrigiano, G. *J. Chem. Soc., Dalton Trans.* **1982**, 2541. (f) Anokhina, E. V.; Jacobson, A. J. *J. Am. Chem. Soc.* **2004**, *126*, 3044. (g) Vaidhyanathan, R.; Bradshaw, D.; Rebilly, J.-N.; Barrio, J. P.; Gould, J. A.; Berry, N. G.; Rosseinsky, M. J. *Angew. Chem., Int. Ed.* **2006**, *45*, 6495. (h) Campana, C. F.; Shepard, D. F.; Litchman, W. M. *Inorg. Chem.* **1981**, *20*, 4039. (i) Dan, M.; Rao, C. N. R. *Chem.—Eur. J.* **2005**, *11*, 7102. (j) Stosick, A. J. *J. Am. Chem. Soc.* **1945**, *67*, 365.